Theoretical Chemistry Accounts (2023) 142:76
https://doi.org/10.1007/s00214-023-03012-w

RESEARCH

New computational tools for chemical kinetics: the *Cathedral Package*

David Ferro-Costas[1] · **Antonio Fernández-Ramos**[1]

Received: 28 February 2023 / Accepted: 13 July 2023 / Published online: 1 August 2023

Abstract
The advent of recent technological developments in software engineering has enabled the exploration of reaction mechanisms inside intricate reaction networks, thereby propelling the beginning of a new era in ab initio kinetics. While it is feasible to consider a substantial number of reactions, determining their rate constants with precision remains an arduous task, even for gas-phase processes. The difficulties are attributed not only to the inherent limitations in the calculation methodology but also to the manual labor and extensive chemical dynamics required, rendering these calculations inaccessible to the general public. As such, there is a pressing need for the development of automated codes and user-friendly interfaces to address this limitation. The present work focuses on the introduction of the *Cathedral package*, a unified computational code comprising the `Q2DTor`, `TorsiFlex`, and `Pilgrim` programs. This package serves to bridge the gap between theoretical studies in chemical kinetics and non-specialist users, making it more accessible and user-friendly.

Keywords Chemical kinetics · Rate constant calculation · Molecular flexibility · Search of conformers · Pilgrim · TorsiFlex · Q2DTor

1 Introduction

For the last few years we have centered our efforts in the study of reactions that occur at very low temperatures, which are relevant in the interstellar medium (ISM) [1–3], and in reactions that take place at high temperatures, as is the case of combustion reactions [4–6]. The theoretical calculation of thermal rate constants is the base to elucidate complex reaction mechanisms in these two extreme regimes. Both situations require a robust theory that incorporates quantum effects into the reactions that occur at very low temperatures, as well as anharmonicity and conformational freedom in flexible molecules at high temperature.

Variational transition state theory (VTST) [7–10] has shown to provide accurate results when compared against fully quantum methods for a large set of atom-diatom reactions [11], and polyatomic systems [12]. The advantage of VTST is that it can be applied to large systems because the rate constant calculations can be performed with a very limited knowledge from the potential energy surface (PES). In most situations, it is enough to evaluate the minimum energy path (MEP) of the reaction [13], together with Hessian calculations at some points along this path. This allows extracting variational and quantum effects employing canonical variational transition state theory (CVT) [14, 15] [which is based on a canonical ensemble (at constant temperature)] with small-curvature tunneling (SCT) corrections [16–18]. Both are ideal approximations to automate thermal rate constant calculations.

For an elementary reaction, the CVT/SCT thermal rate constant is given by:

$$k^{\mathrm{CVT/SCT}}(T) = \gamma^{\mathrm{CVT/SCT}}(T) \cdot B(T) \cdot \frac{Q^{\ddagger}_{\mathrm{rv}}(T)}{Q_{\mathrm{rv,\,R}}(T)} \cdot \exp\left[-\beta V_0\right] \tag{1}$$

where $\gamma(T)$ is the product of two contributions

$$\gamma^{\mathrm{CVT/SCT}}(T) = \Gamma^{\mathrm{CVT}}(T) \cdot \kappa^{\mathrm{CVT/SCT}}(T) \tag{2}$$

being $\Gamma^{\mathrm{CVT}}(T)$ the variational coefficient that accounts for recrossing effects, and $\kappa^{\mathrm{CVT/SCT}}(T)$ the tunneling transmission coefficient calculated by the SCT approximation. Notice

✉ David Ferro-Costas
david.ferro@usc.es

✉ Antonio Fernández-Ramos
qf.ramos@usc.es

[1] Departamento de Química Física y Centro Singular de Investigación en Química Biolóxica e Materiais Moleculares (CIQUS), Universidade de Santiago de Compostela, 15782 Santiago de Compostela, Spain

that $\Gamma^{\mathrm{CVT}}(T) \leq 1$ and $\kappa^{\mathrm{CVT/SCT}}(T) \geq 1$. In the limiting case that both coefficients are the unity CVT/SCT reduces to conventional transition state theory (TST). Therefore, the relation between the CVT/SCT and TST rate constants is

$$k^{\mathrm{CVT/SCT}}(T) = \gamma^{\mathrm{CVT/SCT}}(T) \cdot k^{\mathrm{TST}}(T) \tag{3}$$

and the latter is given by:

$$k^{\mathrm{TST}}(T) = B(T) \cdot \frac{Q^{\ddagger}_{\mathrm{rv}}(T)}{Q_{\mathrm{rv,\,R}}(T)} \cdot \exp\left[-\beta V_0\right] \tag{4}$$

where $\beta = (k_{\mathrm{B}}T)^{-1}$, k_{B} is the Boltzmann's constant and T is the temperature; V_0 is the difference in energy between reactants and the transition state; $Q_{\mathrm{rv,\,R}}(T)$ and $Q^{\ddagger}_{\mathrm{rv}}(T)$ are the rotation-vibration (rovibrational) partition functions of the reactants (R) and the transition state (‡), respectively; and the factor $B(T)$, given by:

$$B(T) = \frac{1}{\hbar\beta}\frac{Q^{\ddagger}_{e}}{Q_{\mathrm{e,R}}}\frac{1}{\Phi_{\mathrm{rel}}(T)} \tag{5}$$

collects Dirac's constant $\hbar$ (Planck's constant divided by 2π), the electronic partition functions, Q_e, of reactants and the transition state, and $\Phi_{\mathrm{rel}}(T)$, which incorporates the relative translational motion of reactants.

In this work, we present the *Cathedral Package* (`CathPkg`) [19], a collection of three programs coded in Python focused on the automated simulation of complex reaction networks consisting in elementary reactions that are analyzed employing VTST. As an additional complication, the stationary points of a set of these elementary reactions may present multiple conformations. Currently, `CathPkg` includes the following programs:

- `Q2DTor` calculates accurate partition functions for molecular systems with two coupled hindered rotors [20].
- `Torsiflex` finds *all* conformations of a given flexible molecule [21, 22].
- `Pilgrim` evaluates the thermal rate constants by VTST and simulates complex reaction networks by Kinetic Monte Carlo (KMC) [23].

In the following sections, we describe how to employ the above programs, to obtain rovibrational partition functions for the stationary points in the case of multiple conformations (multistructural partition functions) [24–29], to incorporate these features into VTST, and to collect this information to simulate kinetic mechanisms.

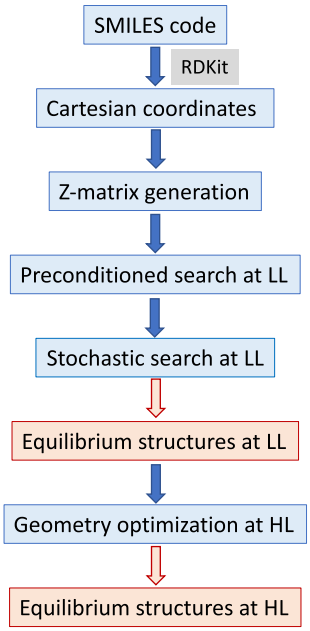

Fig. 1 Scheme showing the flowchart of `Torsiflex`

2 Conformational search

It has been shown that chemical reactions involving molecules with multiple conformations that can be reached by torsional motions are not well represented by a unique structure [24–29], even if this structure corresponds to the absolute minimum. Therefore, prior to the evaluation of a multistructural partition function of a given reactant, we need to carry out a conformational search of all minima that can be reached by internal rotations. The program designated to carry out this task is `Torsiflex`, and the searching procedure is schematically illustrated by the flowchart presented in Fig. 1.

`Torsiflex` reads the SMILES line specification of a given molecular species and transforms it into a Cartesian coordinates geometry with RDKit [30]. From the Cartesian coordinates it is possible to generate, applying Graph Theory, the appropriate Z-Matrix geometry as the input for the electronic structure program. This Z-Matrix specifies the torsions of interest in an unambiguous manner, that is, the internal rotation about a given bond is only specified once. At the moment `Torsiflex` is compatible with *Gaussian*09 [31] and *Gaussian*16 [32], which carry out the geometry optimization.

The searching algorithm combines two strategies: initially, it performs a preconditioned search based on chemical knowledge (for instance, a molecule with two contiguous sp^3 carbon atoms tends to have conformations

at *anti* and *gauche* configurations), subsequently it carries out an stochastic search that maps unexplored regions of the PES. During the search procedure `Torsiflex` runs a series of unexpensive tests that store the new conformers and avoid redundancies [like exploration of regions close to the already located minima or their enantiomers (if any), which are automatically provided by the program]. This search is carried out at a low electronic structure level (LL). All the located conformers are stored and reoptimized at a high level (HL) by the program. The files associated with each conformer can be directly read by `Pilgrim`, which is the program that evaluates the multistructural partition functions.

`Torsiflex` can also be applied to locate conformations of transition state structures. In this case, the construction of the Z-Matrix is more involved. As an example, we have set up a protocol to generate initial transition state structures for hydrogen abstraction reactions from the different isomers of butanol by atomic hydrogen [33].

3 Multistructural rovibrational partition functions

The most common method to treat rotational and vibrational motions, albeit the crudest, is the rigid-rotor harmonic oscillator (RRHO) approximation. The rovibrational partition function for a single-structure, $Q^{\mathrm{SS-HO}}$, is simply the product of the two partition functions[1]:

$$Q^{\mathrm{SS-HO}} = Q_{\mathrm{r}}^{\mathrm{RR}} \cdot Q_{\mathrm{v}}^{\mathrm{HO}} \tag{6}$$

where $Q_{\mathrm{r}}^{\mathrm{RR}}$ and $Q_{\mathrm{v}}^{\mathrm{HO}}$ are the rigid-rotor and harmonic oscillator partition functions for rotation and vibration, respectively.

The natural extension of the RRHO to multiple conformations is to apply this approximation to each of the indistinguishable conformers, leading to the multistructural RRHO partition function, $Q^{\mathrm{MS-HO}}$. For a stationary point with n conformers, it is given by:

$$Q^{\mathrm{MS-HO}} = \sum_{j=0}^{n-1} Q_j^{\mathrm{SS-HO}} \exp\left[-\beta U_j\right] \tag{7}$$

where U_j is the relative energy of the j-th conformer. Notice that, for convenience, the conformers are sorted in increasing order of energy, so $U_0 = 0$ and

$$U_j \leq U_{j'} \quad \forall j < j' \quad | \quad j, j' \in \mathbb{N} \tag{8}$$

It is common to multiply the vibrational frequencies by a parametrized scaling factor [34], λ, that accounts for zero-point energy (ZPE) anharmonicity and is the product of two independent contributions:

$$\lambda = \lambda^{\mathrm{H}} \lambda^{\mathrm{ZPE}} \tag{9}$$

The first contribution on the right-hand side of Eq. 9 reflects the inexactness of the electronic structure method; it is system independent but is determined by both the electronic structure method and the basis set. The second contribution is due to anharmonicity in the ZPE; it is independent of the electronic structure method but system dependent. There are databases with standard values for λ and λ^{H} [35]. However, as λ^{ZPE} is system dependent, its parameterized value may be inadequate for some stationary points (mainly transition state structures) of our particular chemical reaction. Some anharmonicity methods allow incorporating specific reaction scaling factors that provide accurate values for the ZPE anharmonicity. For instance, the hybrid degeneracy-corrected [36] second-order vibrational perturbation theory [37] (HDCVPT2) is a good alternative to the tabulated scaling factors. The latter are parametrized factors that depend on the basis set and the electronic structure method but are independent of the molecular system [35].

The vibrational partition function that incorporates a scaling factor is usually referred as quasi-harmonic (QH). Therefore, the QH partition function is the same as the HO one but with the harmonic normal mode frequencies, ω^{H}, multiplied by the λ scaling factor

$$\omega^{\mathrm{QH}} = \lambda \cdot \omega^{\mathrm{H}} \tag{10}$$

Additionally, the treatment of torsional modes as harmonic oscillators is approximate because the conformers can interconvert between them by internal hindered rotations. For flexible molecules with multiple torsions an accurate treatment of torsional anharmonicity should include the coupling between them. These modes can be separated from the non-torsional modes by transforming the force constants matrix from Cartesian to internal coordinates by employing an adequate set of non-redundant internal coordinates or, in a recent treatment, a set of redundant coordinates [38]. One of the most accurate and inexpensive methods to treat coupled multiple torsions is the multistructural torsional method with coupled potential [MS-T(C)] which only requires information of the conformational minima [29]. Its partition function is given by:

$$Q^{\mathrm{MS-T(C)}} = \sum_{j=0}^{n-1} Q_j^{\mathrm{SS-HO}} F_{\mathrm{cl},j}^{\mathrm{MS-T(C)}} \tag{11}$$

[1] We have removed the rv subscript and added the SS-HO superscript to indicate the single-structure rigid-rotor harmonic oscillator approximation. Hereafter, we also drop the temperature dependence of the partition functions and of the thermal rate constants.

where $F_{\mathrm{cl},j}^{\mathrm{MS-T(C)}}$ is a factor that accounts for the product of the ratios between the reference classical and harmonic oscillator classical partition functions of each of the torsions, η. The former includes torsional anharmonicity and couplings between the torsions so the quotient between partition functions incorporates these deviations from the harmonic oscillator approximation. For a system with t torsions, this is:

$$F_{\mathrm{cl},j}^{\mathrm{MS-T(C)}} = \prod_{\eta=1}^{\mathrm{t}} \frac{q_{j,\eta}^{\mathrm{RC(C)}}}{q_{j,\eta}^{\mathrm{CHO(C)}}} \tag{12}$$

The reference classical partition function approximates the accurate classical partition function considering a local potential about the conformer with just one cosine term. In this case, it is possible to calculate the partition function analytically, so the approximation is very convenient when several torsions are involved.

In systems with only two coupled torsions, it is possible to build an extended two-dimensional torsional (E2DT) partition function [39]. In this method, the rovibrational partition function is the product of two factors

$$Q^{\mathrm{E2DT}} = F^{\mathrm{2D-NS}} Q^{\mathrm{EHR}} \tag{13}$$

The first factor on the right-hand side of Eq. 13 is the ratio between the quantum (q) and classical (cl) two-dimensional non-separable (2D-NS) partition functions:

$$F^{\mathrm{2D-NS}} = \frac{Q_{\mathrm{q}}^{\mathrm{2D-NS}}}{Q_{\mathrm{cl}}^{\mathrm{2D-NS}}} \tag{14}$$

whereas the second factor is the extended hindered rotor (EHR) partition function.

The E2DT partition function can be calculated with the `Q2DTor` program as indicated in Fig. 2. In this case, all calculations are performed at high level. In a first stage, the program performs an scan over the two torsions (usually every 10 degrees) and a partial optimization of the rest of the geometric parameters. The stored geometries are employed to calculate the reduced moments of inertia employing the methodology developed by Kilpatrick and Pitzer [40]. The potential energy (V) and the reduced moments of inertia (I) at these geometries are fitted to Fourier series, so the two-dimensional Schrödinger equation can be solved by the variational method. The calculated energy levels and the resulting wavefunctions can be employed as a tool to extract information about the torsional motion in the molecule.

Specifically, for systems with two or more conformers with the same energy, torsional tunneling splittings are sometimes large enough to be observed, and they can be directly compared with the theoretical results [41–44]. One of us has applied the 2D-NS method to calculate the torsional splitting in benzyl alcohol, 3-fluorobenzyl alcohol, and 4-fluorobenzyl alcohol [45]. For instance, in the case of benzyl alcohol there are 4 minima with the same energy, two of them above the phenyl group ring and two below, and the signals could split into a quadruplet due to the internal rotation. However, only a doublet is observed with a reported splitting of 492.82 MHz [42], and our calculations show that it is due to the rotation of the hydrogen atom of the OH group either above the phenyl group plane or either below that plane. The calculated tunneling splitting amounted to 453 MHz.

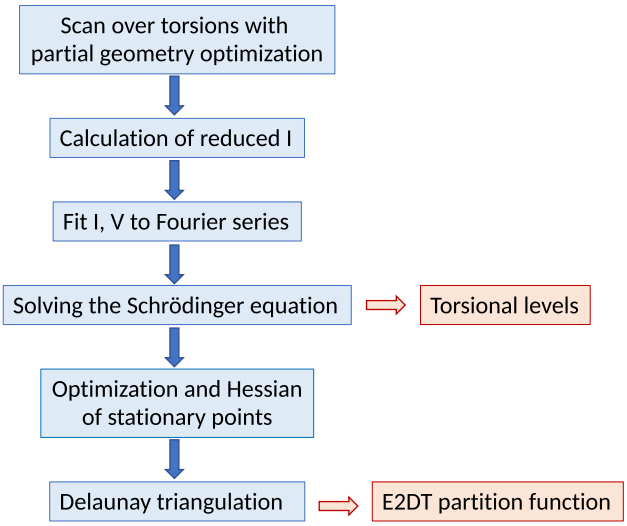

Fig. 2 Scheme showing the flowchart of `Q2DTor`

The evaluation of the E2DT partition function requires a global knowledge of the torsional PES, whereas only local information about the minima is needed in the MS-T(C) method. Therefore, the former method is computationally more demanding than the latter. Both methods can be employed to obtain accurate thermochemical data.

4 Multistructural and multi-path VTST

The multistructural partition functions allow calculating thermal rate constants for reactions that present multiple conformers in both the reactants and the transition state. It is possible to express the multistructural transition state theory (MS-TST) as a function of the single-structure one (SS-TST hereafter, Eq. 4) through a multiplicative factor that accounts for the contribution of conformations:

$$k^{\mathrm{MS-TST}} = F^{\mathrm{MS-QH}} \cdot k^{\mathrm{SS-TST}} \tag{15}$$

where

$$F^{\mathrm{MS-QH}} = \frac{F_{\ddagger}^{\mathrm{MS-QH}}}{F_{\mathrm{R}}^{\mathrm{MS-QH}}} \tag{16}$$

and

$$F_{\mathrm{X}}^{\mathrm{MS-QH}} = \frac{Q_{\mathrm{X}}^{\mathrm{MS-QH}}}{Q_{\mathrm{X}}^{\mathrm{SS-QH}}} \tag{17}$$

where X = R or ‡ stands for reactants or the transition state, respectively.

Therefore, the multistructural QH version of TST is:

$$k^{\mathrm{MS-TST}} = F^{\mathrm{MS-QH}} \cdot B(T) \cdot \frac{Q_{\ddagger}^{\mathrm{SS-QH}}}{Q_{\mathrm{R}}^{\mathrm{SS-QH}}} \exp\left[-\beta V_0\right] \tag{18}$$

where the single-structure partition functions refer to the absolute minimum of reactants and the most stable structure of the transition state, and V_0 is the barrier height between them. Equation 18 can also be written as:

$$k^{\mathrm{MS-TST}} = B(T) \cdot \frac{Q_{\ddagger}^{\mathrm{MS-QH}}}{Q_{\mathrm{R}}^{\mathrm{MS-QH}}} \exp\left[-\beta V_0\right] \tag{19}$$

For the anharmonic (Anh) version of MS-TST we introduce another factor F^{Anh} that accounts for torsional anharmonicity, and it is given by:

$$F^{\mathrm{Anh}} = \frac{F_{\ddagger}^{\mathrm{Anh}}}{F_{\mathrm{R}}^{\mathrm{Anh}}} \tag{20}$$

and

$$F_{\mathrm{X}}^{\mathrm{Anh}} = \frac{Q_{\mathrm{X}}^{\mathrm{Anh}}}{Q_{\mathrm{X}}^{\mathrm{MS-QH}}} \tag{21}$$

where the method to include torsional anharmonicity could be, for instance, MS-T(C) or E2DT. Notice that $Q_{\mathrm{X}}^{\mathrm{Anh}}$ is also a quasi-harmonic partition function [see Eqs (9) and (10)] to which we have added torsional anharmonicity.

Therefore, the anharmonic version of MS-TST can be written as:

$$k_{\mathrm{Anh}}^{\mathrm{MS-TST}} = F^{\mathrm{Anh}} \cdot k^{\mathrm{MS-TST}} \tag{22}$$

or as a function of the SS-TST:

$$k_{\mathrm{Anh}}^{\mathrm{MS-TST}} = F^{\mathrm{Anh}} \cdot F^{\mathrm{MS-QH}} \cdot k^{\mathrm{SS-TST}} \tag{23}$$

The procedure to obtain the rate constants by Eq. 23 consists of the following steps:(i) executing `Torsiflex` to locate all conformers of the reactants and the transition state; (ii) running `MsTor` to obtain the MS-T(C) partition functions; and (iii) running `Pilgrim` to calculate the MS-TST thermal rate constants. For systems with just two torsions, steps (i) and (ii) can be substituted by executing `Q2DTor`.

The next step is to incorporate variational and SCT tunneling effects into the MS-TST rate constant. On the one hand, if we consider that these two effects are well represented by the ones obtained by employing the transition state conformation with the lowest energy ($\gamma_0^{\mathrm{CVT/SCT}}$), we have the multistructural CVT/SCT rate constant (MS-CVT/SCT), which is given by:

$$k^{\mathrm{MS-CVT/SCT}} = \gamma_0^{\mathrm{CVT/SCT}} k^{\mathrm{MS-TST}} \tag{24}$$

On the other hand, if variational and tunneling effects are calculated for each of the $n^{\ddagger}$ transition state structures, we have the multi-path CVT/SCT rate constant (MP-CVT/SCT), which is given by:

$$k^{\mathrm{MP-CVT/SCT}} = \langle \gamma^{\mathrm{CVT/SCT}} \rangle \cdot k^{\mathrm{MS-TST}} \tag{25}$$

where $\langle \gamma^{\mathrm{CVT/SCT}} \rangle$ represents the Boltzmann average of the variational and tunneling contributions of each of the transition state structures, that is,

$$\langle \gamma^{\mathrm{CVT/SCT}} \rangle = \sum_{j_{\ddagger}=0}^{n^{\ddagger}-1} \Gamma_{j_{\ddagger}}^{\mathrm{CVT}} \kappa_{j_{\ddagger}}^{\mathrm{CVT/SCT}} \chi_{j_{\ddagger}}^{\mathrm{QH}} \tag{26}$$

where the Boltzmann factor for the $j^{\ddagger}$-th transition state structure is given by:

$$\chi_{j_{\ddagger}}^{\mathrm{QH}} = \frac{Q_{j_{\ddagger}}^{\mathrm{SS-QH}}}{Q_{\ddagger}^{\mathrm{MS-QH}}} e^{-\beta U_{j_{\ddagger}}} \tag{27}$$

`Pilgrim` can deal with all these flavors of variational transition state theory following the scheme displayed in Fig. 3. Once the MS-TST rate constant is calculated, the MEP is run starting from just the lowest TST, so the MS-CVT/SCT rate constant is obtained, or is run starting on each of the transition state structures, so the MP-CVT/SCT rate constant can be calculated.

4.1 Kinetic isotope effects

`Pilgrim` can also be used to evaluate kinetic isotope effects (KIEs) within multi-path variational transition state theory. For instance, we have analyzed different deuterium substitutions in the ethanol molecule employing this methodology and our calculated results were in good agreement with experiment [46, 47]. Ethanol presents two distinguishable conformers and the hydrogen/deuterium abstraction by atomic hydrogen/deuterium also leads to several transition state conformations. For a given isotopic substitution, the KIE is simply:

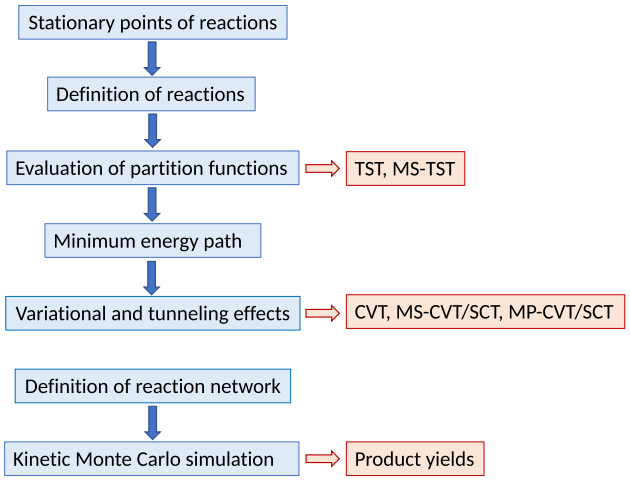

Fig. 3 Scheme showing the flowchart of `Pilgrim`

$$\eta^{\mathrm{MP-CVT/SCT}} = \frac{k_{\mathrm{H}}^{\mathrm{MP-CVT/SCT}}}{k_{\mathrm{D}}^{\mathrm{MP-CVT/SCT}}} \tag{28}$$

where $k_{\mathrm{H}}^{\mathrm{MP-CVT/SCT}}$ and $k_{\mathrm{D}}^{\mathrm{MP-CVT/SCT}}$ are the MP-CVT/SCT rate constants for the root and isotopically substituted species, respectively. It is possible to analyze the contribution of each transition state conformer to the final KIE by employing the following expression:

$$\eta^{\mathrm{MP-CVT/SCT}} = \sum_{j_{\ddagger}=0}^{n^{\ddagger}-1} \eta_{j_{\ddagger}} \tag{29}$$

where $\eta_{j_{\ddagger}}$ accounts for the contribution of each reaction path to the total KIE. Each of these individual contributions can be split as a product of a weighting factor that depends exclusively on the isotopic substitution and an individual transition state contribution to the KIE. `Pilgrim` provides the MP-CVT/SCT thermal rate constants for each of the isotopes, as well as the resulting KIEs.

5 Kinetic Monte–Carlo

Typically, a reaction mechanism encompasses various elementary steps, denoted as R_i. With the aid of `Pilgrim`, it is possible to evaluate the rate constant of each elementary step separately and track the system's evolution over time using the kinetic Monte Carlo (KMC) algorithm. It relies on Gillespie's direct method [48, 49], and can be employed to determine the branching ratios of products and its temperature dependence. This is particularly advantageous in investigations involving numerous elementary reactions, such as those encountered in combustion processes. For example, we have applied this method to examine the thermal decomposition of 1-propanol radicals in one of our studies [6].

The propensity function, a_i, linked to each elementary reaction, R_i, depends on the current population of the reaction reactant(s) and the corresponding rate constant. Precisely, in the infinitesimal time interval $[t, t + dt]$, $a_i dt$ signifies the likelihood, at time t, that reaction R_i will transpire within a particular volume V. During every step of the KMC simulation, a distinct elementary step R_i is selected, and the population of the involved species are modified, assuming that a given time (τ) has elapsed.

The reaction is selected employing the nonuniform distribution of propensities with tower sampling, which is a rejection-free approach. More explicitly, for a single random number $r_1 \in [0, 1]$, the algorithm selects the R_i reaction that meets the following condition:

$$\sum_{j=1}^{i-1} a_j < r_1 \cdot \sum_{j=1}^{} a_j \leq \sum_{j=1}^{i} a_j \tag{30}$$

The elapsed time is determined by a second single random number, $r_2 \in [0, 1]$, through:

$$\tau = -\frac{\log(r_2)}{\sum_{i=1} a_i} \tag{31}$$

The `Pilgrim` program executes the algorithm either until the population of the initial reactive species is depleted or until the population of each species reaches the equilibrium.

6 Conclusion

We have devoted our efforts to the development of integrated computational codes that enable non-expert users to perform theoretical studies on chemical kinetics. Our accomplishment, the *Cathedral package*, is accessible on Github [19] and comprises the following programs:

- `Torsiflex`, which identifies all the conformational isomers of flexible acyclic molecules;
- `Q2DTor`, which employs the extended two-dimensional torsional (E2DT) approach to handle torsional anharmonicity in flexible molecules with two coupled torsions; and
- `Pilgrim`, which utilizes direct-dynamics to compute thermal rate constants of chemical reactions and simulates chemical kinetics mechanisms.

These programs can be applied in numerous fields such as organometallic catalysis, gas-phase mass spectrometry, the simulation of microwave spectra, the calculation of thermodynamic properties, and the study of several chemical

reactions that occur in the gas phase. In our research, we concentrate on utilizing these codes for combustion chemistry and the study of processes occurring at ultra-low temperatures.

Acknowledgements The authors thank "Centro de Supercomputación de Galicia" (CESGA) for the use of their computational facilities. This work was partially supported by the Consellería de Cultura, Educación e Ordenación Universitaria (Centro singular de investigación de Galicia acreditación 2019-2022, ED431G 2019/03 and Grupo de referencia competitiva ED431C 2021/40) and the European Regional Development Fund (ERDF), and the Ministerio de Ciencia e Innovación through Grant PID2019-107307RB-I00. D.F.-C. thanks Xunta de Galicia for financial support through a postdoctoral grant.

Funding Open Access funding provided thanks to the CRUE-CSIC agreement with Springer Nature.

Declarations

Conflict of interest There are no conflict of interest to declare.

References

1. Siebrand W, Smedarchina Z, Martínez-Núñez E, Fernández-Ramos A (2016) Methanol dimer formation drastically enhances hydrogen abstraction from methanol by OH at low temperature. Phys Chem Chem Phys 18:22712–22718
2. Gao L, Zheng J, Fernández-Ramos A, Truhlar DG, Xu X (2018) Kinetics of the methanol reaction with OH at interstellar, atmospheric, and combustion temperatures. J Am Chem Soc 140:2906–2918
3. González D, Lema-Saavedra A, Espinosa S, Martínez-Núñez E, Ramos AF, Canosa A, Ballesteros B, Jiménez E (2022) Reaction of OH radicals with CH_3NH_2 in the gas phase: experimental (11.7-177.5 K) and computed rate coefficients (10–1000 K). Phys Chem Chem Phys 24:23593–23601
4. Meana-Pañeda R, Truhlar DG, Fernández-Ramos A (2011) High-level direct-dynamics variational transition state theory calculations including multidimensional tunneling of the thermal rate constants, branching ratios, and kinetic isotope effects of the hydrogen abstraction reactions from methanol by atomic hydrogen. J Chem Phys 134(9):0943202
5. Meana-Pañeda R, Fernández-Ramos A (2014) Accounting for conformational flexibility and torsional anharmonicity in the H + CH_3CH_2OH hydrogen abstraction reactions: A multi-path variational transition state theory study. J Chem Phys 140:174303
6. Ferro-Costas D, Martínez-Núñez E, Rodríguez-Otero J, Cabaleiro-Lago E, Estévez CM, Fernández B, Fernández-Ramos A, Vázquez SA (2018) Influence of multiple conformations and paths on rate constants and product branching ratios. thermal decomposition of 1-propanol radicals. J. Phys. Chem. A 122, 4790–4800
7. Garrett BC, Truhlar DG (1980) Variational transition-state theory. Acc Chem Res 13:440–448
8. Truhlar DG, Isaacson AD, Garrett BC (1985). In: Baer M (ed) Theory of chemical reaction dynamics, 2nd edn. CRC, Boca Raton
9. Fernández-Ramos A, Ellingson A, Garrett BC, Truhlar DG (2007) Variational transition state theory. Rev Comput Chem 23:125–262
10. Bao JL, Truhlar DG (2017) Variational transition state theory: theoretical framework and recent developments. Chem Soc Rev 46:7548–7596
11. Allison TC, Truhlar DG (1998). In: Thompson DL (ed) Testing the accuracy of practical semiclassical methods: modern methods for multidimensional dynamics computations in chemistry. World Scientific, Singapore, pp 618–712
12. Pu JZ, Truhlar DG (2002) Validation of variational transition state theory with multidimensional tunneling contributions against accurate quantum mechanical dynamics for H+CH_4 → H_2+CH_3 in an extended temperature interval. J Chem Phys 117(4):1479–1481
13. Melissas VS, Truhlar DG, Garrett BC (1992) Optimized calculations of reaction paths and reaction-path functions for chemical reactions. J Chem Phys 96:5758–5772
14. Garrett BC, Truhlar DG (1979) Criterion of minimum state density in the transition state theory of bimolecular reactions. J Chem Phys 70(4):1593–1598
15. Garrett BC, Truhlar DG (1979) Generalized transition state theory. Classical mechanical theory and applications to collinear reactions of hydrogen molecules. J Phys Chem 83:1052–1078
16. Skodje RT, Truhlar DG, Garrett BC (1982) Vibrationally adiabatic models for reactive tunneling. J Chem Phys 77:5955–5976
17. Lu D-H, Truong TN, Melissas VS, Lynch GC, Liu Y-P, Garrett BC, Steckler R, Isaacson AD, Rai SN, Hancock GC, Lauderdale JG, Joseph T, Truhlar DG (1992) Polyrate 4: a new version of a computer program for the calculation of chemical reaction rates for polyatomics. Comput Phys Commun 71:235–262
18. Liu Y-P, Lynch GC, Truong TN, Lu D-H, Truhlar DG (1993) Molecular modeling of the kinetic isotope effect for the [1,5]-sigmatropic rearrangement of cis-1,3-pentadiene. J Am Chem Soc 115:2408–2415
19. Ferro-Costas D, Fernández-Ramos A (2021) The cathedral package. https://github.com/cathedralpkg (Accessed January 24, 2023)
20. Ferro-Costas D, Cordeiro MNDS, Truhlar DG, Fernández-Ramos A (2018) Q2DTor: a program to treat torsional anharmonicity through coupled pair of torsions in flexible molecules. Comput Phys Commun 232:190–205
21. Ferro-Costas D, Fernández-Ramos A (2020) A combined systematic-stochastic algorithm for the conformational search in flexible acyclic molecules. Front Chem 8:16
22. Ferro-Costas D, Mosquera-Lois I, Fernández-Ramos A (2021) Torsiflex: an automatic generator of torsional conformers. Application to the twenty proteinogenic amino acids. J Cheminform 13:100
23. Ferro-Costas D, Truhlar DG, Fernández-Ramos A (2020) Pilgrim: a thermal rate constant calculator and a chemical kinetics simulator. Comput Phys Commun 256:107457
24. Meana-Pañeda R, Fernández-Ramos A (2012) Tunneling and conformational flexibility play critical roles in the isomerization mechanism of vitamin D. J Am Chem Soc 134:346–354
25. Zheng J, Truhlar DG (2012) Multi-path variational transition state theory for chemical reaction rates of complex polyatomic species: ethanol + OH reactions. Faraday Discuss 157:59–88
26. Zheng J, Yu T, Papajak E, Alecu IM, Mielke SL, Truhlar DG (2011) Practical methods for including torsional anharmonicity in

thermochemical calculations on complex molecules: The internal-coordinate multi-structural approximation. Phys Chem Chem Phys 13:10885–10907
27. Yu T, Zheng J, Truhlar DG (2011) Multi-structural variational transition state theory. Kinetics of the 1,4-hydrogen shift isomerization of the pentyl radical with torsional anharmonicity. Chem Sci 2:2199–2213
28. Zheng J, Yu T, Truhlar DG (2011) Multi-structural thermodynamics of C–H bond dissociation in hexane and Isohexane yielding seven isomeric hexyl radicals. Phys Chem Chem Phys 13:19318–19324
29. Zheng J, Truhlar DG (2013) Quantum thermochemistry: multistructural method with torsional anharmonicity based on a coupled torsional potential. J Chem Theory Comput 9:1356–1367
30. Landrum G (2021) RDKit: Open-source cheminformatics and machine learning. http://www.rdkit.org
31. Frisch MJ, Trucks GW, Schlegel HB, Scuseria GE, Robb MA, Cheeseman JR, G. Scalmani Barone V, Mennucci B, Petersson GA, Nakatsuji H, Caricato M, Li X, Hratchian HP, Izmaylov AF, Bloino J, Zheng G, Sonnenberg JL, Hada M, Ehara M, Toyota K, Fukuda R, Hasegawa J, Ishida M, Nakajima T, Honda Y, Kitao O, Nakai H, Vreven T, Montgomery Jr, JA, Peralta JE, Ogliaro F, Bearpark M, Heyd JJ, Brothers E, Kudin KN, Staroverov VN, Kobayashi R, Normand J, Raghavachari K, Rendell A, Burant JC, Iyengar SS, Tomasi J, Cossi M, Rega N, Millam JM, Klene M, Knox JE, Cross JB, Bakken V, Adamo C, Jaramillo J, Gomperts R, Stratmann RE, Yazyev O, Austin AJ, Cammi R, Pomelli C, Ochterski JW, Martin RL, Morokuma K, Zakrzewski VG, Voth GA, Salvador P, Dannenberg JJ, Dapprich S, Daniels AD, Farkas O, Foresman JB, Ortiz JV, Cioslowski J, Fox DJ, (2009) Gaussian 09. Gaussian Inc, Wallingford
32. Frisch MJ, Trucks GW, Schlegel HB, Scuseria GE, Robb MA, Cheeseman JR, Scalmani G, Barone V, Petersson GA, Nakatsuji H, Li X, Caricato M, Marenich AV, Bloino J, Janesko BG, Gomperts R, Mennucci B, Hratchian HP, Ortiz JV, Izmaylov AF, Sonnenberg JL, Williams-Young D, Ding F, Lipparini F, Egidi F, Goings J, Peng B, Petrone A, Henderson T, Ranasinghe D, Zakrzewski VG, Gao J, Rega N, Zheng G, Liang W, Hada M, Ehara M, Toyota K, Fukuda R, Hasegawa J, Ishida M, Nakajima T, Honda Y, Kitao O, Nakai H, Vreven T, Throssell K, Montgomery JA Jr, Peralta JE, Ogliaro F, Bearpark MJ, Heyd JJ, Brothers EN, Kudin KN, Staroverov VN, Keith TA, Kobayashi R, Normand J, Raghavachari K, Rendell AP, Burant JC, Iyengar SS, Tomasi J, Cossi M, Millam JM, Klene M, Adamo C, Cammi R, Ochterski JW, Martin RL, Morokuma K, Farkas O, Foresman JB, Fox DJ (2016) Gaussian 16, Revision A-03. Gaussian Inc, Wallingford
33. Ferro-Costas D, Cordeiro MNDS, Fernández-Ramos A (2022) An integrated protocol to study hydrogen abstraction reactions by atomic hydrogen in flexible molecules: application to butanol isomers. Phys Chem Chem Phys 24:3043–3058
34. Pople JA, Scott AP, Wong MW, Radom L (1993) Scaling factors for obtaining fundamental vibrational frequencies and zero-point energies from HF/6-31G* and MP2/6-31G* harmonic frequencies. Isr J Chem 33:345–350
35. Alecu IM, Zheng J, Zhao Y, Truhlar DG (2010) Computational thermochemistry: scale factor databases and scale factors for vibrational frequencies obtained from electronic model chemistries. J Chem Theory Comput 6:2872–2887
36. Kuhler KM, Truhlar DG, Isaacson AD (1996) General method for removing resonance singularities in quantum mechanical perturbation theory. J Chem Phys 104:4664–4671
37. Bloino J, Biczysko M, Barone V (2012) General perturbative approach for spectroscopy, thermodynamics, and kinetics: methodological background and benchmark studies. J Chem Theory Comput 8:1015–1036
38. Chen W, Zhang P, Truhlar DG, Zheng J, Xu X (2022) Identification and treatment of internal rotation in normal mode vibrational analysis. J Chem Theory Comput 18:7671–7682
39. Simón-Carballido L, Bao JL, Alves TV, Meana-Pañeda R, Truhlar DG, Fernández-Ramos A (2017) Anharmonicity of coupled torsions: the extended two-dimensional torsion method and its use to assess more approximate methods. J Chem Theory Comput 13:3478–3492
40. Kilpatrick JE, Pitzer KS (1949) Energy levels and thermodynamics functions for molecules with internal rotation. iii compound rotation. J Chem Phys 17:1064–1075
41. Evangelisti L, Gou Q, Feng G, Caminati W (2013) Effects of ring fluorination on the transient atropisomerism of benzyl alcohol: the rotational spectrum of 3,4-difluorobenzyl alcohol. Mol Phys 111(14):1994–1998
42. Utzat KA, Bohn RK, Montgomery JA, Michels HH, Caminati W (2010) Rotational spectrum, tunneling motions, and potential barriers of benzyl alcohol. J Phys Chem A 114(25):6913
43. Tang S, Xia Z, Maris A, Caminati W (2010) Tunnelling splittings in the rotational spectrum of 3-fluoro-benzylalcohol. Chem Phys Lett 498:52–55
44. Bird RG, Nikolaev AE, Pratt DW (2011) Microwave and UV excitation spectra of 4-fluorobenzyl alcohol at high resolution. S_0 and S_1 structures and tunneling motions along the low frequency $-CH_2OH$ torsional coordinate in both electronic states. J Phys Chem A 115:11369–11377
45. Alves TV, Simón-Carballido L, Ornellas FR, Fernández-Ramos A (2016) Hindered rotor tunneling splittings: an application of the two-dimensional non-separable method to benzyl alcohol and two of its fluorine derivatives. Phys Chem Chem Phys 18:8945–8953
46. Simón-Carballido L, Alves TV, Dybala-Defratyka A, Fernández-Ramos A (2016) Kinetic isotope effects in multipath VTST: application to a hydrogen abstraction reaction. J Chem Phys B 120:1911–1918
47. Kannath S, Adamczyk P, Ferro-Costas D, Fernández-Ramos A, Major DT, Dybala-Defratyka A (2020) The role of microsolvation and quantum effects in the accurate prediction of kinetic isotope effects: the case of hydrogen atom abstraction in ethanol by atomic hydrogen in aqueous solution. J Chem Theory Comput 16:847–859
48. Gillespie DT (1976) A general method for numerically simulating the stochastic time evolution of coupled chemical reactions. J Comput Chem 22:403–434
49. Gillespie DT (2007) Stochastic simulation of chemical kinetics. Annu Rev Phys Chem 58:35–55